

## SYNTHESIS AND CHARACTERIZATION OF Ni-NH<sub>2</sub>/MESOPOROUS SILICA CATALYST FROM LAPINDO MUD FOR HYDROCRACKING OF WASTE COOKING OIL INTO BIOFUEL

W. Trisunaryanti\*, Triyono, C. Paramesti, S. Larasati, N. R. Santoso,  
and D. A. Fatmawati

<sup>1</sup>Department of Chemistry, Faculty of Mathematics and Natural Sciences,  
Universitas Gadjah Mada, Sekip Utara Bulaksumur, Yogyakarta 55281, Indonesia

\*E-mail: [wegats@ugm.ac.id](mailto:wegats@ugm.ac.id)

### ABSTRACT

The synthesis and characterization of Ni-NH<sub>2</sub>/Mesoporous Silica (MS) catalysts from Lapindo mud for the hydrocracking of waste cooking oil into biofuel has been conducted. The MS was synthesized by the hydrothermal method using CTAB as a template. The functionalization of -NH<sub>2</sub> into MS was carried out by the grafting method. The Ni metal was loaded into NH<sub>2</sub>/MS by wet impregnation. The catalytic activity test was done for hydrocracking of waste cooking oil by using the MS, NH<sub>2</sub>/MS, and Ni-NH<sub>2</sub>/MS catalysts. The results of the liquid product of the hydrocracking were analyzed by the gravimetric method and GC-MS. The experimental result showed that the liquid products of the hydrocracking using MS, NH<sub>2</sub>/MS, and Ni-NH<sub>2</sub>/MS catalysts were 63.95, 70.32, and 66.44 wt.%. The highest selectivity of the gasoline fraction (34.98 wt.%) was produced by the NH<sub>2</sub>/MS catalyst and the highest diesel oil fraction (1.52 wt.%) was produced by MS. The NH<sub>2</sub>/MS catalyst was successfully used as a catalyst in the hydrocracking of waste cooking oil into the hydrocarbons (biofuel).

**Keywords:** Biofuel, CTAB, Lapindo mud, Mesoporous silica, Ni-NH<sub>2</sub>

© RASĀYAN. All rights reserved

### INTRODUCTION

Energy supply within the future is an issue that pulls the consideration of all countries because human welfare in advanced life is closely related to the amount and quality of energy utilized. At current production rates, Indonesia's saves for crude oil are assessed to last for 23 years.<sup>1,2</sup> The transportation and industrial sectors become the highest energy consumers followed by the household sector. Due to Indonesia's rapid consumption in oil and natural gas reserves, the country must find an alternative energy source to maintain economic development within the future.<sup>3</sup>

Biofuels offer any guarantees on these frontiers since they offer benefits to natural effects in comparison to fossil fuels<sup>4</sup>. One of the biofuel sources is waste cooking oil because this will be accommodated for the reduction of environmental contamination. This conversion will be a valuable addition of energy in the existing energy grid<sup>5</sup>.

During the frying process, oil persistently degenerates when exposed to high temperature, oxygen, and moisture so it leads to physical and chemical changes including the formation of hydrolysis products such as free fatty acids (FFAs)<sup>6</sup>. To convert FFA into biofuel compounds, meso-sized material is required as a great adsorption medium.

The mesoporous materials have attracted the attention of numerous researchers in different application fields<sup>7</sup>. The choice of basic mesoporous material is critical because it acts as a building block. One of the main ingredients that are superior is silica since it has properties that are thermally stable, safe, and inexpensive<sup>8</sup>. Pure silica materials are MCM, SBA, HMS, whereas the non-silica mesoporous materials incorporate transition metal oxides<sup>9</sup>.

Silica can be found in natural materials, including Lapindo mud<sup>10</sup>. Lapindo mud is the result of an erupting mud volcano in the subdistrict of Porong, Sidoarjo in East Java, Indonesia. Lapindo mud can be the main source of material in the synthesis of mesoporous because of high silica content (>47%). Hence, Lapindo mud has enormous potential as one of the advancement sources of silica production<sup>11</sup>.

One of the main variables of the mesoporous material synthesis is the determination of the template. The primary requirement for a template is to have the amphiphilic and shaping mesostructure characters<sup>12</sup>. The type of surfactant that often used is a cationic surfactant, which is cetyltrimethylammoniumbromide (CTAB)<sup>13</sup>. The addition of CTAB produces materials with more amount of interconnected pores, and thus, the specific surface area increases<sup>14</sup>.

Mesoporous silica (MS) is a silica material gotten by hydrothermal synthesis by the mechanism of liquid templating<sup>7</sup>. MS material is uncharged so that it can be used as a catalyst in the hydrocracking process. Catalyst activity with transition metal adjustment on the carrier solids has been widely examined and appears great activity and selectivity since its Lewis acid sites<sup>15</sup>. Marsuki et al. (2018)<sup>16</sup> effectively synthesized Co-Mo/Mesoporous silica-alumina which were utilized as catalysts for hydrocracking of  $\alpha$ -cellulose.

In present, MCM-41 functionalized by amine group ( $\text{NH}_2$ ) is a heterogeneous catalyst and can catalyze many of organic reaction<sup>17</sup>. One of them is the basic catalyst in the transesterification of VCO (fresh) to produced methyl ester<sup>18</sup>. Ifah et al. (2016)<sup>19</sup> have been functionalized MCM-41 with an amine group by the addition of 3-aminopropyltrimetoxysilane (3-APTMS) into MCM-41- $\text{NH}_2$  for transesterification of waste palm oil.

The activity of the bifunctional catalyst has already studied and has shown a good activity and selectivity, one of them is Ni- $\text{NH}_2$ /MS. The adsorbent-catalyst hybrid nanostructured material which consisted of aminopropyl and nickel nanoparticles moved into MS and specifically work; the amino group binds with FFA in microalgae oil and nickel-metal converts it into saturated hydrocarbons<sup>20</sup>. However, MS was prepared using tetramethylorthosilicate (TMOS) and a nonionic block copolymer Pluronic P104 surfactant. Based on the explanation, the novelty of this research is  $\text{NH}_2$  and Ni- $\text{NH}_2$  will be loaded into the MS which is synthesized from silica of Lapindo mud and CTAB template, as well as the correlation between the character of the catalysts and catalytic activity for hydrocracking of waste cooking oil in producing liquid fraction and selectivity to gasoline and diesel oil fraction.

## EXPERIMENTAL

### Materials

The material used in this experiment were silica extracted from Lapindo mud, hydrochloric acid (HCl 37%), sodium hydroxide (NaOH), nickel nitrate hexahydrate ( $\text{Ni}(\text{NO}_3)_2 \cdot 6\text{H}_2\text{O}$ ), silver nitrate ( $\text{AgNO}_3$ ), Cetyltrimethylammoniumbromide (CTAB), 3-Aminopropyltrimethoxysilane (3-APTMS), toluene, methanol, universal pH paper, distilled water,  $\text{N}_2$  and  $\text{H}_2$  gas, ammonia ( $\text{NH}_3$ ), Whatman No. 42 and 41, and waste cooking oil.

### Synthesis of Mesoporous Silica by CTAB

For the synthesis of mesoporous silica (MS) by the CTAB template, 3.18 g of CTAB was mixed with 65 mL of distilled water by hot plate stirrer at 40 °C. The homogenized solution was put on the PET glass. Then, 6 g of silica extracted Lapindo mud ( $\text{SiO}_2$  content of 96.86 wt.%) and 200 mL of NaOH 1.5 M were mixed, so the  $\text{Na}_2\text{SiO}_3$  was formed. CTAB solution was dripped by  $\text{Na}_2\text{SiO}_3$  solution bit by bit while the solution was mixed until it homogenized and waited for 1 h. The solution was added by HCl 3M until pH 11 was reached and awaited for 4 h. The solution was put into the autoclave at 100 °C for 24 h. The formed white solid was washed by distilled water until it neutralized. The solid was dried at 80 °C for 24 h. The MS was produced, 0.5 g was saved for being the MS sample before the calcination process. The rest of MS was calcined for 5 h at 450 °C with the 5 °C/minute for temperature increment. The calcined MS was characterized by FTIR and SAA.

### Grafting of Amine Group in Mesoporous Silica

For the amine group grafting in MS, 3-APTMS was dissolved in 20 mL of toluene. The solution was refluxed at 90 °C for 20 minutes. 0.5 g of MS catalyst was added into the solution. The solution was

refluxed for 5 h at 90 °C. The solution was centrifuged in 2000 rpm for 20 minutes. The solid was washed by toluene for one time and it washed by methanol two times with centrifugation separation. The result was put into the oven at 50 °C for 24 h. The NH<sub>2</sub>/MS catalyst was characterized by FTIR and SAA.

### Impregnation of Nickel Metal on NH<sub>2</sub>/MS

The 4 wt.% of Ni metal was loaded into the 1 g of NH<sub>2</sub>/MS by wet impregnation method using a salt precursor of Ni(NO<sub>3</sub>)<sub>2</sub>·6H<sub>2</sub>O and dissolved by 50 mL of distilled water. The solution was stirred by magnetic stirrer at 300 rpm for 24 h. The mixture was evaporated at 70 °C. The solid was gassed by N<sub>2</sub> and calcined at 500 °C for 1 h. The sample was reduced by H<sub>2</sub> gas (15 cm<sup>3</sup>/minute) at 450 °C for 3 h. The catalysts produced were Ni-NH<sub>2</sub>/MS. The catalyst was characterized by FTIR, SAA, and TEM.

### Catalytic Activity Test

The catalysts and the waste cooking oil were put to the conversion reactor and into the furnace with hydrocracking technique with the ratio between the weight of catalyst/waste cooking oil was 1/50 (w/w). The variation of catalysts was MS, NH<sub>2</sub>/MS, and Ni-NH<sub>2</sub>/MS. After that, the catalysts were calcined at 450 °C with a temperature increment of 10 °C/minute and with the H<sub>2</sub> gas flow rate of 15 mL/minute. The product of hydrocracking was flowed through the cooler and placed into the flask. The result of the hydrocracking process was determined by the percentage (%) of the liquid product conversion by using the equation below:

$$\text{Liquid (wt.\%)} = \frac{W_l}{W_f} \times 100\%$$

$$\text{Coke (wt.\%)} = \frac{W_{c1} - W_{c0}}{W_f} \times 100\%$$

$$\text{Gas (wt.\%)} = 100\% - (\text{liquid} + \text{coke})$$

Hydrocracking results were analyzed by GC-MS. The chromatogram was showed the relative percentages for each compound contained in the liquid product. Gasoline fraction was a hydrocarbon compound composed of alkanes with C<sub>5</sub>-C<sub>12</sub> carbon number and diesel oil fractions composed of C<sub>13</sub>-C<sub>17</sub> carbon chains. Determination of percent selectivity of gasoline fraction and the diesel oil fraction to liquid products by waste cooking oil can be determined by using the equations below:

$$\text{Gasoline fraction (\%)} = \frac{\text{Relative E\% C}_5\text{-C}_{12}}{\% \text{Total relative}} \times \text{Liquid Product (\%)}$$

$$\text{Diesel oil fraction (\%)} = \frac{\text{Relative E\% C}_{13}\text{-C}_{17}}{\% \text{Total relative}} \times \text{Liquid Product (\%)}$$

**Note** : E% = GC area (%)  
 W<sub>l</sub> = Weight of the liquid product  
 W<sub>f</sub> = Weight of feed  
 W<sub>c0</sub> = Weight of catalyst before hydrocracking  
 W<sub>c1</sub> = Weight of catalyst after hydrocracking

### Detection Method

The functional groups of all samples were determined using Fourier Transform Infrared Spectrometer (FTIR, Shimadzu Prestige-21). The surface parameters (surface area, pore-volume, and pore diameter) of the samples were analyzed using the Surface Area Analyzer (SAA, Quantachrome NovaWin2 1200e version 2.2). The pore images were taken using a Transmission Electron Microscope (TEM, JEOL JEM-1400). The liquid products obtained from hydrocracking of waste cooking oil were analyzed using Gas Chromatography-Mass Spectrometry (GC-MS, Shimadzu QP2010S).

## RESULTS AND DISCUSSION

### Analysis of Fourier Transform Infra-Red (FTIR)

Based on the FTIR spectra of the pure silica in (1a), there were four highest pure silica typical functional groups could be seen which indicated the formation of the silica network. They are the stretching vibration of Si-OH of at 3448.72 cm<sup>-1</sup>, the bending vibration of Si-OH at 1635.64 cm<sup>-1</sup>, and the Si-O-Si vibration at 1095.57 cm<sup>-1</sup> and 470.63 cm<sup>-1</sup>.

Furthermore, it also can be seen that there were significant differences in the certain region of wavenumber between MS before (1b) and after (1c) calcination. Both of them showed the Si-OH group at  $3448.72\text{ cm}^{-1}$  and  $1640\text{ cm}^{-1}$ , the asymmetric stretching of the Si-O-Si at  $1072.42\text{ cm}^{-1}$ , symmetric stretching of the Si-O-Si at  $810\text{ cm}^{-1}$ , and the symmetrical bending of Si-O-Si at  $480\text{ cm}^{-1}$ . The highest peak of each wavenumber is indicated that synthesized MS by the hydrothermal method has already formed. After the calcination, the appearance of three peaks (the symmetrical stretching vibration of the C-H  $\text{sp}_3$  group at  $2924.09\text{ cm}^{-1}$ , the asymmetrical stretching vibration of the C-H  $\text{sp}_2$  group at  $2854.65\text{ cm}^{-1}$ , and the bending vibration and vibration from the N-H and C-H groups at  $1473.62\text{ cm}^{-1}$ ) belongs to CTAB template in the IR spectra of MS has been lost or reduced. The CTAB is unstable and easily degraded or lost by high temperatures. This indicates that the calcination process has been done successfully.

The additional amine group to the MS and Ni/MS has aimed to minimize the possibility of leaching in the catalysts and capture the FFA compounds contained in waste cooking oil. Based on (1d) and (1e) it can be shown that the functional groups of 3-APTMS compounds qualitatively appeared at an absorption peak of  $2931.80\text{ cm}^{-1}$  (the vibration group of  $\text{CH}_2$ ) and  $1527\text{ cm}^{-1}$  (the vibration group of  $\text{NH}_2$ ). The spectra of both the samples showed low absorption intensity because of the low amount of 3-APTMS concentration, which is 5%. The result has shown that the modification of MS and Ni/MS by 3-APTMS successfully carried out.

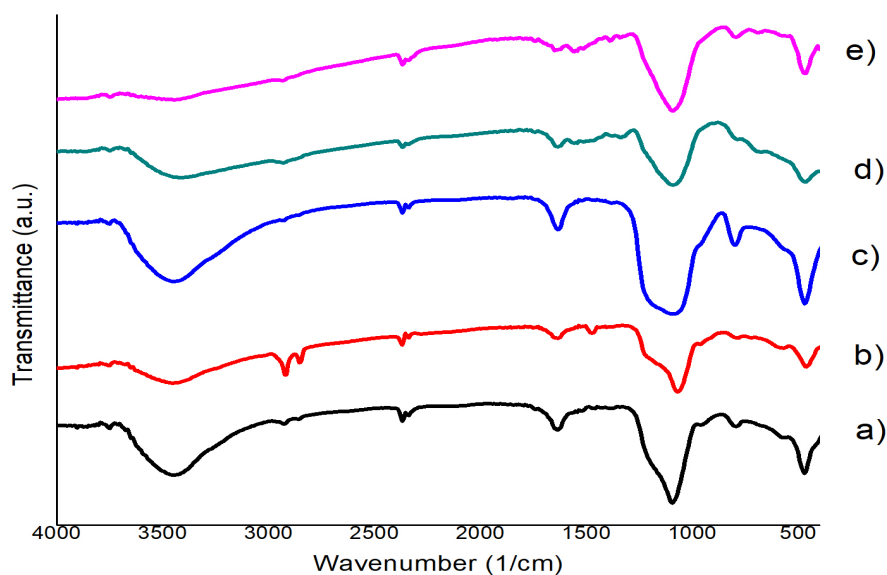


Fig.-1: FTIR Spectra of (a) Pure Silica, (b) MS before Calcination, (c) MS after Calcination, (d)  $\text{NH}_2$ -MS, (e)  $\text{Ni-NH}_2/\text{MS}$

### Analysis of Surface Area Analyzer (SAA)

Analysis of the surface in this experiment using surface area analyzer (SAA) instrument included specific surface area, pore diameter, total pore volume, pore type, and pore distribution.

The result of the isotherm is shown in Fig.-2, the adsorption-desorption isotherm curve of all materials from the synthesis is approached the Type IV pattern. According to IUPAC (1985), type IV isotherms are generally adsorbents that tend to occur through multilayer formation followed by capillary condensation and usually occurred in mesoporous material<sup>21</sup>.

Hysteresis loops are formed because of the capillary condensation of the mesoporous which is appeared in the different relative pressure. The appearance of hysteresis loops by the capillary condensation in the mesoporous structure showed that all materials already synthesized. The hysteresis loops pattern also gives a certain meaning, (2a) it has H1 type hysteresis loops which exhibit a narrow range of uniform

mesopores, usually, network effects are minimal and the steep, narrow loop is a clear sign of delayed condensation on the adsorption branch. Meanwhile, (2b) it has H2 type which has very steep desorption branch and can be attributed either to pore-blocking/percolation in a narrow range of pore necks or cavitation-induced evaporation, and (2c) it has H4 type which is somewhat similar, but the adsorption branch is now a composite of types I and II, the more pronounced uptake at low  $p/p_0$  being associated with the filling of micropores<sup>22</sup>.

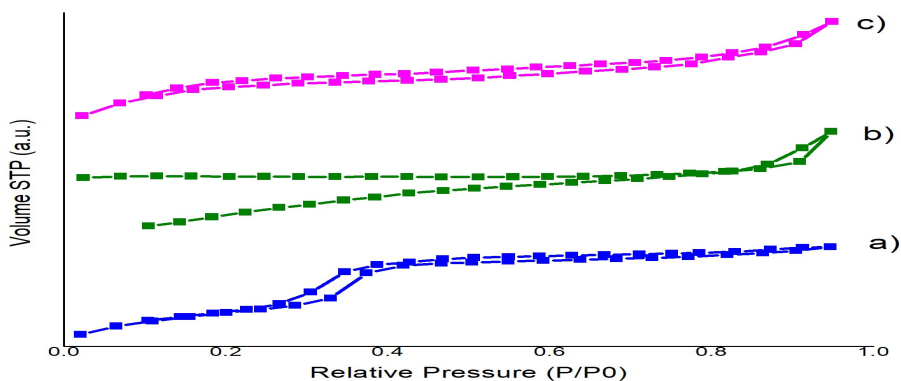


Fig.-2: Nitrogen Gas Adsorption-Desorption Isotherms of (a) MS, (b)  $\text{NH}_2/\text{MS}$ , (c)  $\text{Ni-NH}_2/\text{MS}$

Figure-3 showed the pore distribution of materials measured by BJH (Barrett-Joyner-Halenda) desorption. The materials which can be classified as mesoporous material has a pore diameter between 2-50 nm based on the IUPAC classification. The specific surface of pore diameter and total pore volume as the structure parameter of the  $\text{NH}_2/\text{MS}$  and  $\text{Ni-NH}_2/\text{MS}$  catalyst presented in Table-1.

Table-1: Parameter of Materials Structure

Catalyst	Specific Surface Area ( $\text{m}^2/\text{g}$ ) <sup>a</sup>	Pore Diameter (nm) <sup>b</sup>	Total Pore Volume ( $\text{cc/g}$ ) <sup>c</sup>
MS	874.284	3.59368	0.814090
$\text{NH}_2/\text{MS}$	6.25083	3.26868	0.053386
$\text{Ni-NH}_2/\text{MS}$	13.6482	3.90532	0.013667

Note: <sup>a</sup> Specific Surface Area measured with BET

<sup>b</sup> Pore diameter measured with BJH desorption

<sup>c</sup> Total Pore Volume determined from nitrogen adsorption in relative pressure (0.99)

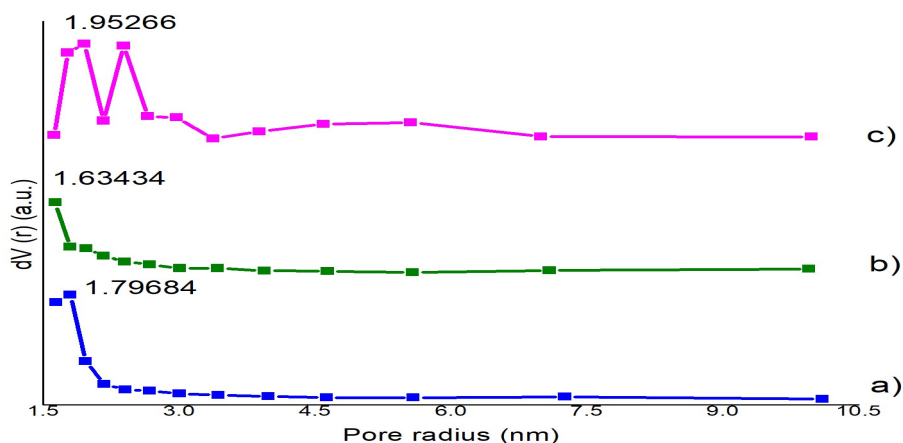


Fig.-3: Pore Distribution Curves of (a) MS, (b)  $\text{NH}_2/\text{MS}$ , (c)  $\text{Ni-NH}_2/\text{MS}$

Based on the Table-1, MS has a very large surface area, but after grafting the molecule  $-\text{NH}_2$  into MS, the surface area of the catalyst drops dramatically. This is possible because these molecules cover or block

the pores inside the mesoporous material. Furthermore, after impregnation of Ni metals, the surface area will increase again, although not sharply. This is possible because Ni metals adhere at the surface of the material thereby increasing the contact field between the substrate and the catalyst material. The increase and decrease in the surface area followed by pore diameter. The pore diameter showed the highest pore distribution.

#### Analysis of Transmission Electron Microscope (TEM)

The TEM micrograph of the Ni-NH<sub>2</sub>/MS in Fig.-4 showed that the dark part shows the presence of solid as a pore wall, while the bright part shows the absence of solid as hollow space. Furthermore, the pore size of the Ni-NH<sub>2</sub>/MS is not uniform. The catalyst has a wormhole-like pore structure.

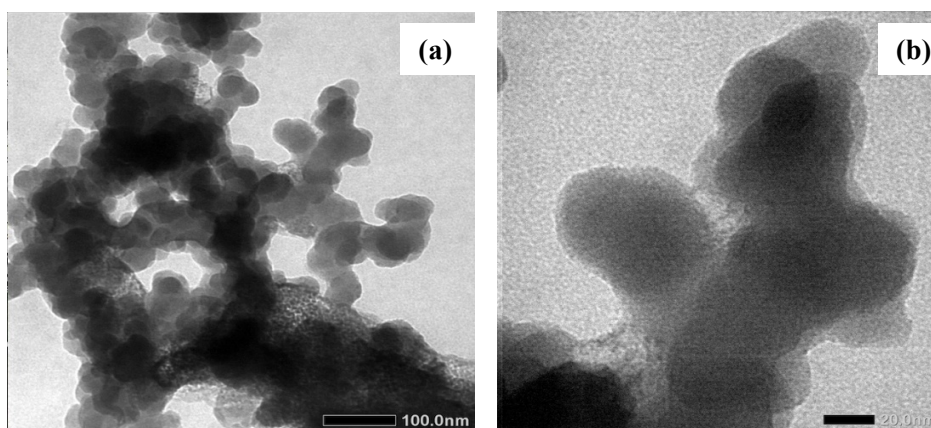


Fig.-4: TEM Images of the Ni-NH<sub>2</sub>/MS with Micron Marker of (a) 100 nm and (b) 20 nm

#### Catalytic Activity Test

The activities of MS, NH<sub>2</sub>/MS, and Ni-NH<sub>2</sub>/MS catalysts were evaluated in a hydrocracking reaction. The analysis was using quantitative analysis where the percentage of the products from the hydrocracking process were calculated. The products were including the main product, coke, and gas. The liquid sample from the catalysts is being tested for selectivity. The hydrocracking of waste cooking oil into hydrocarbon fraction (biofuel) is shown in Table-2. In the hydrocracking of MS, the liquid product that produced is 63.95 wt.%. While in the use of NH<sub>2</sub>/MS and Ni-NH<sub>2</sub>/MS, the liquid products that produced are 70.32 wt.% and 66.44 wt.%. NH<sub>2</sub>/MS showed the highest catalytic activity, so the catalyst can be used to increase the liquid product.

Table-2: Conversion of Waste Cooking Oil

Catalyst	Conversion (wt.%)		
	Liquid	Gas	Coke
MS	63.95	30.33	5.72
NH <sub>2</sub> /MS	70.32	27.74	1.94
Ni-NH <sub>2</sub> /MS	66.44	30.00	3.56

The hydrocracking of liquid products is then analyzed by using GC-MS to find out the estimated compounds produced in the waste cooking oil of the hydrocracking process. The content of each gasoline fraction (C<sub>5</sub>-C<sub>12</sub>), diesel fraction (C<sub>13</sub>-C<sub>17</sub>), and organic in the hydrocracking liquid product can be known from the percentage of peak area of the GC-MS test results. Table-3 showed the fractions of the liquid products produced in the hydrocracking of waste cooking oil.

Table-3 showed that the result of the catalytic activity test by heating at the temperature of 450 °C on the hydrocracking of waste cooking oil into a shorter hydrocarbon chain. Based on the table, the selectivity of NH<sub>2</sub>/MS catalyst in the hydrocracking of waste cooking oil produced a dominant gasoline fraction of 34.98 wt.%, while the highest diesel fraction selectivity that is produced from SM catalyst is 1.52 wt.%. This is indicated that the NH<sub>2</sub>/MS catalyst can capture the free fatty acid (FFA) as well as it can make cracking into shorter hydrocarbons. Thus, the type of catalyst in the hydrocracking of waste cooking oil



can affect the selectivity of liquid products to the gasoline fraction and the diesel fraction that is produced. Based on the explanation, it showed that the  $\text{NH}_2/\text{MS}$  has the highest catalytic activity because almost the big part of the hydrocracking of the waste cooking oil process is produced hydrocarbon compounds.  $\text{NH}_2/\text{MS}$  material was successfully used as a catalyst in the hydrocracking of waste cooking oil into the hydrocarbons (biofuel).

Table-3: Data of Hydrocracking of Liquid Product Based on the Fractions

Catalyst	The Fraction in a Liquid Product (wt.%)			
	Gasoline Fraction ( $\text{C}_5\text{-C}_{12}$ ) <sup>a</sup>	Diesel Fraction ( $\text{C}_{13}\text{-C}_{17}$ ) <sup>b</sup>	Organic	Total of Liquid Product
MS	20.96	1.52	41.64	63.95
$\text{NH}_2/\text{MS}$	34.98	0.72	34.62	70.32
$\text{Ni-NH}_2/\text{MS}$	21.91	1.40	41.57	66.44

Note : <sup>a</sup> Gasoline fraction measured from (% area ( $\text{C}_5\text{-C}_{12}$ )/ 100% x %liquid product  
<sup>b</sup> Diesel oil fraction measured from (% area ( $\text{C}_{13}\text{-C}_{17}$ )/ 100% x %liquid product  
<sup>c</sup> Organic fraction measured from (% area (organic)/ 100% x %liquid product

### CONCLUSION

1. The mesoporous silica (MS) has structure characteristics as a porous material with pore diameter, specific surface area, and pore volume respectively 3.59368 nm, 874.284  $\text{m}^2/\text{g}$ , and 0.81409  $\text{cm}^3/\text{g}$ .
2. The specific surface area of  $\text{NH}_2/\text{MS}$  and  $\text{Ni-NH}_2/\text{MS}$  catalysts are 6.25083 and 13.6482  $\text{m}^2/\text{g}$ ; where the pore diameters are 3.26868 and 3.90532 nm; and the total volumes are 0.053386 and 0.013667  $\text{cc}/\text{g}$ .
3. The liquid product of waste cooking oil hydrocracking by using MS,  $\text{NH}_2/\text{MS}$ , and  $\text{Ni-NH}_2/\text{MS}$  catalysts are 63.95, 70.32, and 66.44 wt.%. The highest selectivity of the gasoline fraction (34.98 wt.%) produced by the  $\text{NH}_2/\text{MS}$  catalyst and the highest diesel fraction (1.52 wt.%) produced by MS catalysts.  $\text{NH}_2/\text{MS}$  material was successfully used as a catalyst in the hydrocracking of waste cooking oil into the hydrocarbons (biofuel).

### ACKNOWLEDGMENT

The author thanks The Indonesian Ministry of Research, Technology, and Higher Education, the Republic of Indonesia for Financial support under the scheme of PDUPT research grant 2020 (Contract Number: 2806/UN1.DITLIT/DIT-LIT/PT/2020).

### REFERENCES

1. M. H. Hasan, T. M. I. Mahlia, and H. Nur, *Renewable and Sustainable Energy Reviews*, **16**(4), 2316(2012), DOI: 10.1016/j.rser.2011.12.007
2. Handbook of energy and economic statistic of Indonesia. Jakarta, Indonesia: Ministry of Energy and Mineral Resources, (2010)
3. W. Trisunaryanti, I.I. Falah, D.R. Prihandini, and M.F. Marsuki, *Rasayan Journal of Chemistry*, **12**(3), 1523(2012), DOI: 10.31788/RJC.2019.1235297
4. A. Pandey, C. Larroche, S.C.Ricke, C.G. Dussap, and E. Gnansounou, *Biofuels: Alternative Feedstocks and Conversion Processes*, Academic Press, Oxford (2011)
5. L. Brennan and P. Owende, *Renewable and Sustainable Energy Reviews*, **14**(2), 557(2010), DOI: 10.1016/j.rser.2009.10.009
6. N. Bazina and J. He, *Journal of Food Science and Technology*, **55**(8), 3085(2018), DOI: 10.1007/s13197-018-3232-9
7. W. Trisunaryanti, Triyono, I.I. Falah, A.D. Siagian, and M.F. Marsuki, *Indonesian Journal Chemistry*, **18**(3), 441(2018), DOI: 10.22146/ijc.31717
8. W. Trisunaryanti, Triyono, and D. A. Fatmawati, *Rasayan Journal of Chemistry*, **13**, 723(2020), DOI:10.31788/RJC.2020.1315514
9. S. Kumar, M.M. Malik, and R. Purohit, *Materials Today: Proceedings*, **4**(2), 350(2017), DOI: 10.1016/j.matpr.2017.01.032
10. I. B. P. Mahardika, W. Trisunaryanti, Triyono, D. P. Wijaya, and K. Dewi, *Indonesian Journal of Chemistry*, **17**(3), 509(2017), DOI:10.22146/ijc.26561

11. H. Kusumastuti, W. Trisunaryanti, I.I. Falah, and M.F. Marsuki, *Rasayan Journal of Chemistry*, **11(2)**, 522(2018), DOI:10.31788/RJC.2018.112206
  12. A. Masykuroh, W. Trisunaryanti, I.I. Falah, and Sutarno, *International Journal of ChemTech Research*, **9**, 598(2016).
  13. Ma, Yong, C. Zhang, C. Hou, H. Zhang, H. Zhang, Q. Zhang, and Z. Guo, *Polymer*, **117**, 30(2017), DOI:10.1016/j.polymer.2017.04.010
  14. N.I. Vazquez, Gonzalez, B. Ferrari, and Y. Castro, *Boletín de la Sociedad Española de Cerámica y Vidrio*, **56(3)**, 139(2017), DOI:10.1016/j.bsecv.2017.03.002
  15. W. Trisunaryanti, *Material Katalis dan Karakternya*, Gadjah Mada University Press, Yogyakarta (2014)
  16. M.F. Marsuki, W. Trisunaryanti, I.I. Falah, and K. Wijaya, *Oriental Journal Chemistry*, **34**, 955(2018), DOI:10.13005/ojc/340245
  17. D.B. Nale, S. Rana, K. Parida, and B.M. Bhanage, *Applied Catalysis A: General*, **469**, 340(2014), DOI:10.1016/j.apcata.2013.10.011
  18. T. Triyono, H.M. Khoiri, W. Trisunaryanti, and K. Dewi, *IOSR Journal of Applied Chemistry*, **8(8)**, 50(2015), DOI: 10.9790/5736-08825056
  19. A.A. Ifah, W. Trisunaryanti, Triyono, and K. Dewi, *International Journal of ChemTech Research*, **9**, 382(2016).
  20. K. Kandel, C. Frederickson, E.A. Smith, Y.J. Lee, and I.I. Slowing, *ACS Catalysis*, **3**, 2750-2758 (2013), DOI: 10.1021/cs4008039
  21. Triyono, W. Trisunaryanti, A.D. Putri and K. Dewi, *Asian Journal of Chemistry*, **30(5)**, 954 (2018), DOI:10.14233/ajchem.2018.20979
  22. M. Thommes, K. Kaneko, A.V. Neimark, J.P. Olivier, F. Rodriguez-Reinoso, J. Rouquerol, and K.S.W. Sing, *Pure and Applied Chemistry*, **87(9-10)**, 1(2015), DOI:10.1515/pac-2014-1117
- [RJC-5840/2020]